

Supplemental Figure Legends

Supplemental Figure S1. Assessment of Acrosome Reaction of Sperm with Cumulus-Oocyte Complexes. To assess the physiological acrosome reaction relevant to IVF we observed the acrosome status of sperm within COC. Sperm DNA was stained with Hoechst 33342 (blue) before IVF and used to count total sperm within the COC. Alexa 488-conjugated soybean trypsin inhibitor (green) was used to mark sperm with reacted acrosomes. Images were collected at 250X magnification.

Supplemental Figure S2. Detection of Hydrogen Peroxide in Mouse Sperm Using Boronate Small Molecule Probes. Hydrogen peroxide specific boronate probes with different targeting groups were used to measure hydrogen peroxide in a variety of cellular contexts. Images were collected at 630X magnification. **A)** Intracellular hydrogen peroxide was detected with PF6-AM. **B)** MitoPY1 was used to detect hydrogen peroxide production from sperm mitochondria. **C)** PG1 is a cell permeable hydrogen peroxide probe, which is also active in the extracellular media. Cryopreserved sperm are stained over the entirety of the membrane, and fluorescence is present in the surrounding media as well.

Supplemental Figure S3. Total H₂O₂, Intracellular H₂O₂, and Lipid Peroxidation of the Sperm Principal Piece Do Not Correlate with IVF Rate. **A)** Total H₂O₂ levels of cryopreserved B6/J sperm suspensions, assessed by plate reader measurement of PG1 fluorescence. Mouse strains responded differently to CD and antioxidants in a manner not corresponding to IVF rate. **B)** Measurements of intracellular levels of viable cryopreserved B6/J sperm by flow cytometry. B6129XF1, B6/J, and B6/N intracellular H₂O₂ levels were elevated by cryopreservation. CD elevated intracellular H₂O₂ of B6/J and 129X1 above cryopreservation alone, and GSH reduced B6/J intracellular H₂O₂. **C)** Principal piece lipid peroxidation is increased in cryopreserved 129X1 sperm relative to the FVB/NJ ($p < 0.05$), and reduced by CD and MTG. GSH reduced B6/J and B6/N principal piece lipid peroxidation, and CD additionally reduced it in B6/N. Four biological replicates were performed for each group and data are represented as the mean \pm SEM. *, **, ***, # indicate $p < 0.05$, 0.01, 0.001, 0.001 respectively by two-tailed, unpaired t-test compared to cryopreserved sperm of the same mouse strain.

Supplemental Figure S4. Total Sperm Number is Consistent Among Strains After Cryopreservation and Zona Pellucida Binding Varies on the Basis of Mouse Strain in a Manner Unassociated with IVF Rate. **A)** Sperm binding of the zona pellucida of the oocyte was higher for B6129XF1 and B6/J sperm than FVB/NJ and 129X1. **B)** Total sperm within COC after 30 minutes of co-incubation is similar among all strains after cryopreservation. Four biological replicates were performed for each group.

Supplemental Figure S5. Motility Parameters of Cryopreserved B6/J Sperm Are Unaffected by CD and Antioxidants. CASA assessment shows of percent motility and CASAnova classification of progressive and hyperactivated sperm motility patterns are not altered by CD or antioxidants. Data are represented as the mean \pm SEM of four biological replicates.

Supplemental Figure S6. Combinations of CD and Antioxidants Do Not Improve IVF Rates of Cryopreserved B6/J Sperm More than Antioxidants Alone and CD Diminishes the Protective

Effect of Antioxidants on H₂O₂ Production. We investigated the ability of combinations of antioxidants and CD to further improve IVF rates A), but we found the combination did not produce IVF rates higher than antioxidants alone. When we analyzed the intracellular B) and mitochondrial C) H₂O₂ production of cryopreserved B6/J sperm incubated with antioxidants and CD we found the protective effects of antioxidants were diminished or eliminated, potentially accounting for IVF rates remaining unchanged. Data are represented as the mean \pm SEM of four biological replicates. *, **, ***, # indicate $p < 0.05, 0.01, 0.001, 0.001$, respectively, by two-tailed, unpaired t-test compared to cryopreserved sperm alone.

Supplemental Figure S1

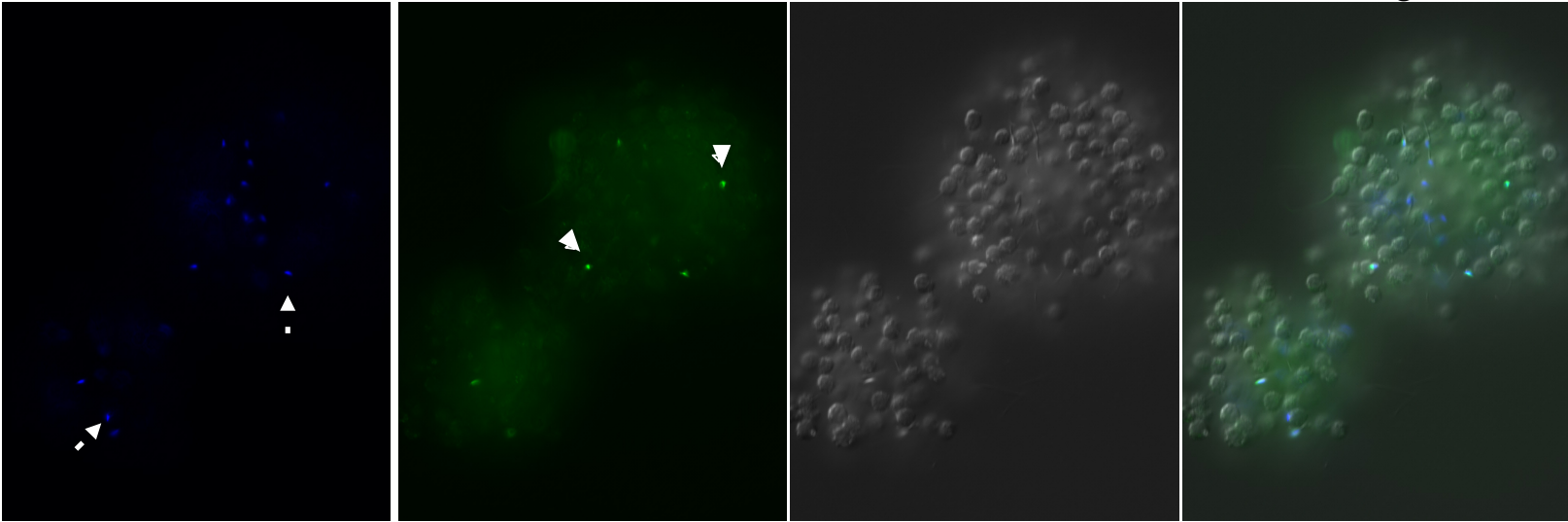
A

Hoechst 33342

Soybean Trypsin
Inhibitor Alexa
488 Conjugate

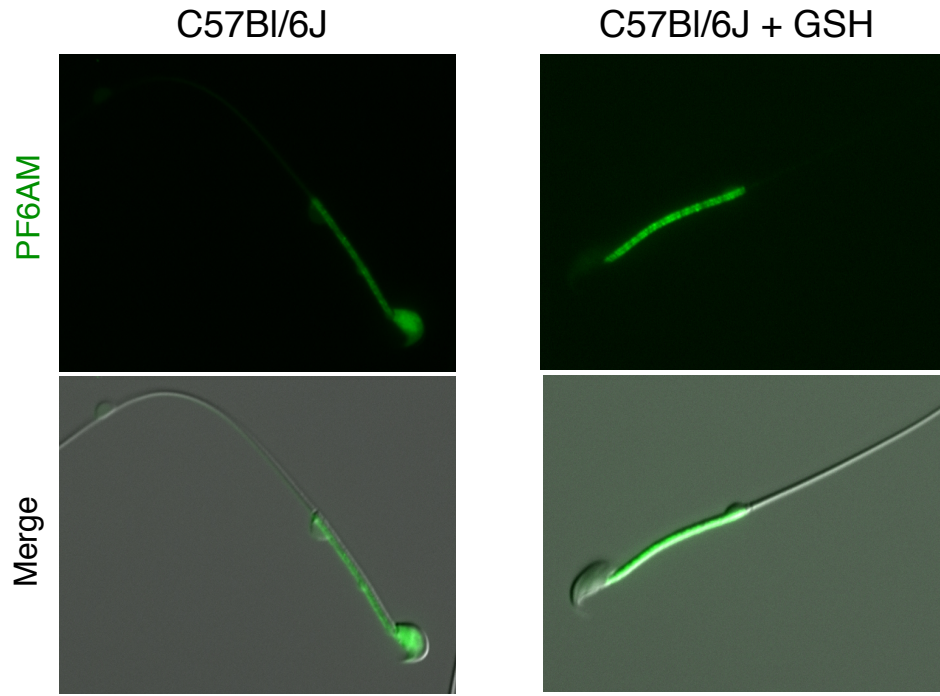
DIC

Merge

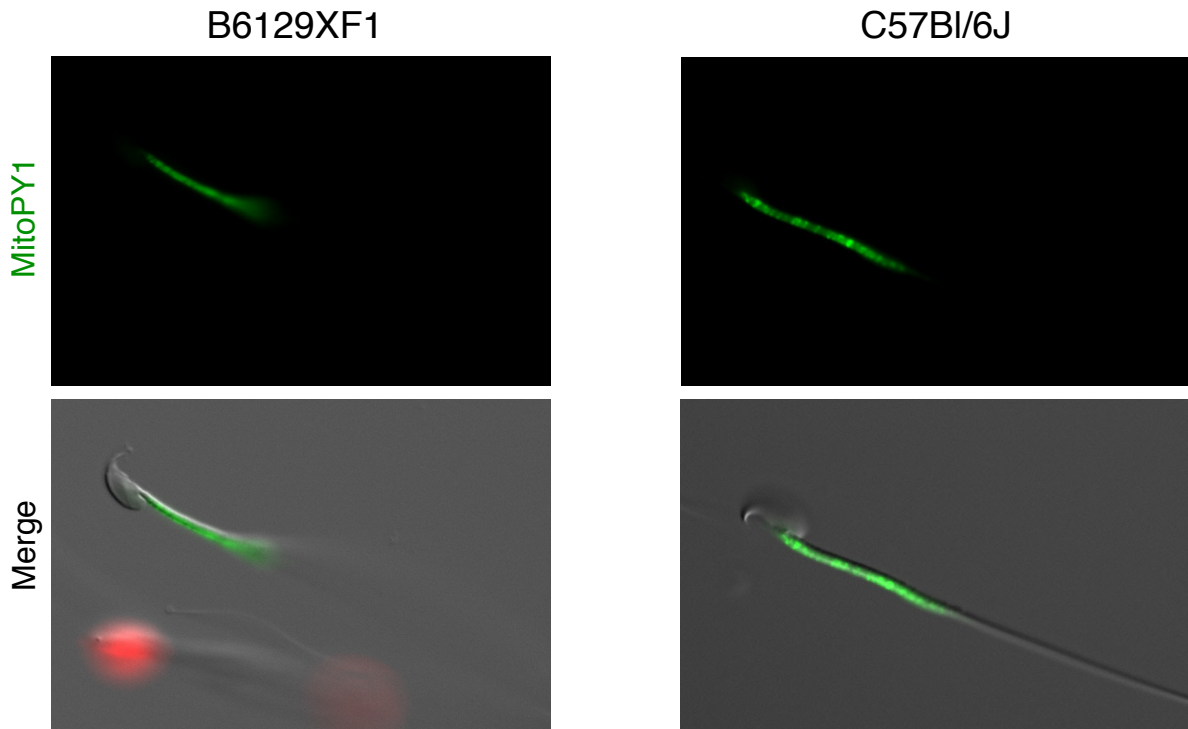


Supplemental Figure S2

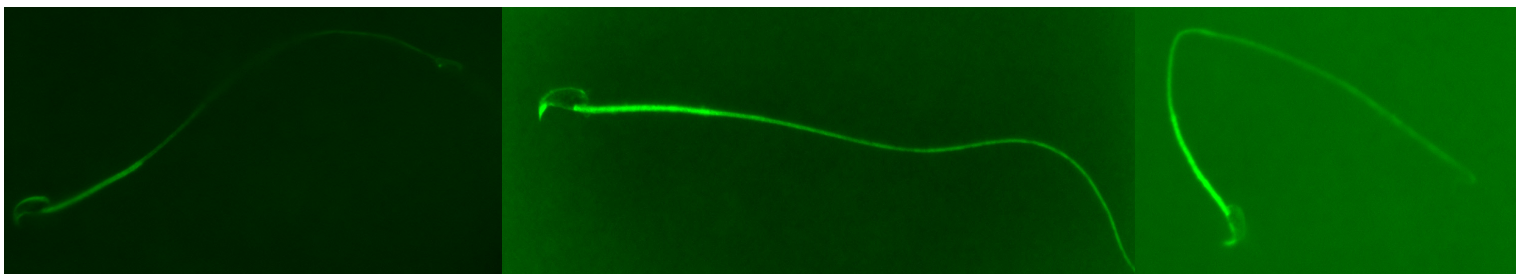
A



B

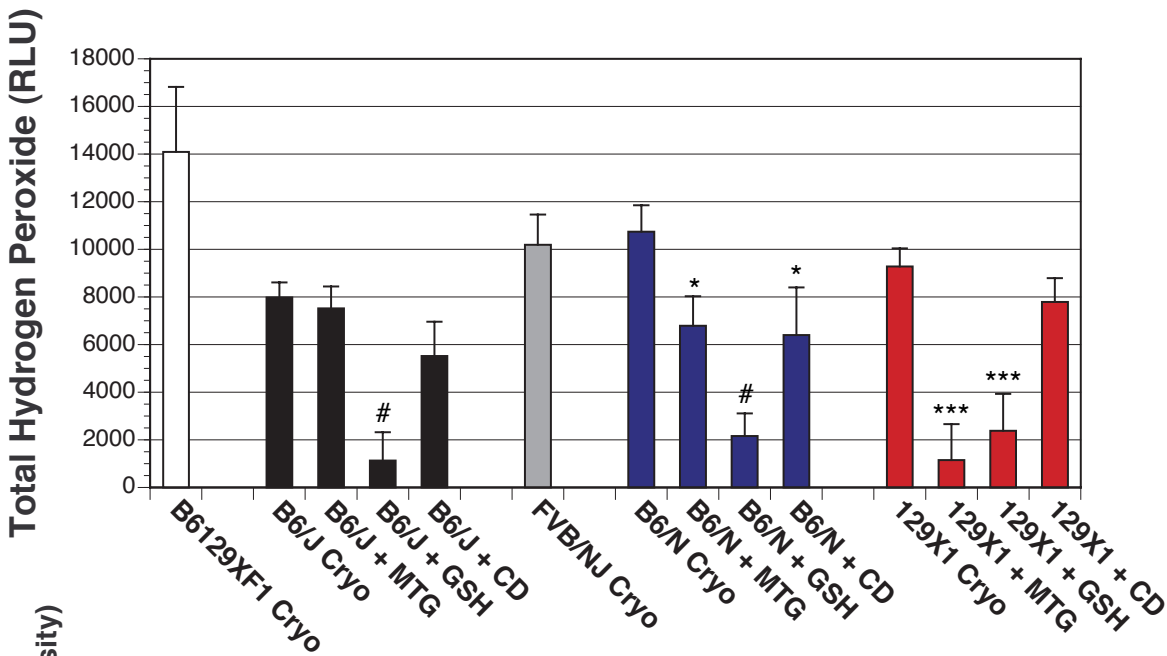


C

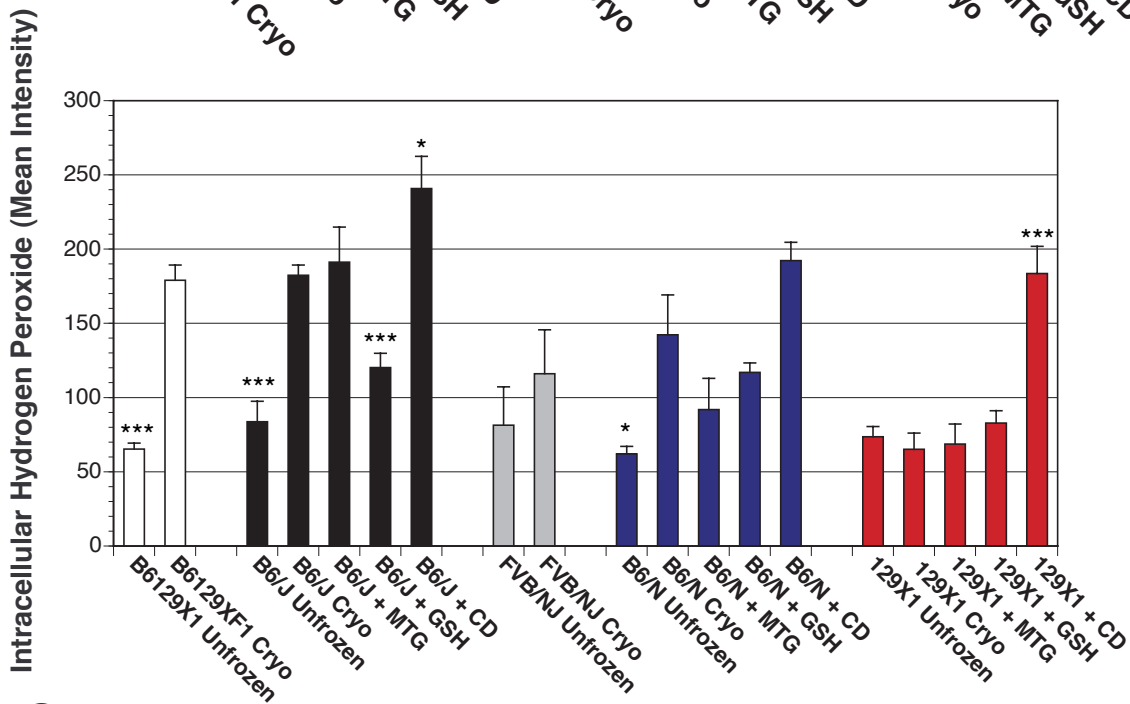


Supplemental Figure 3

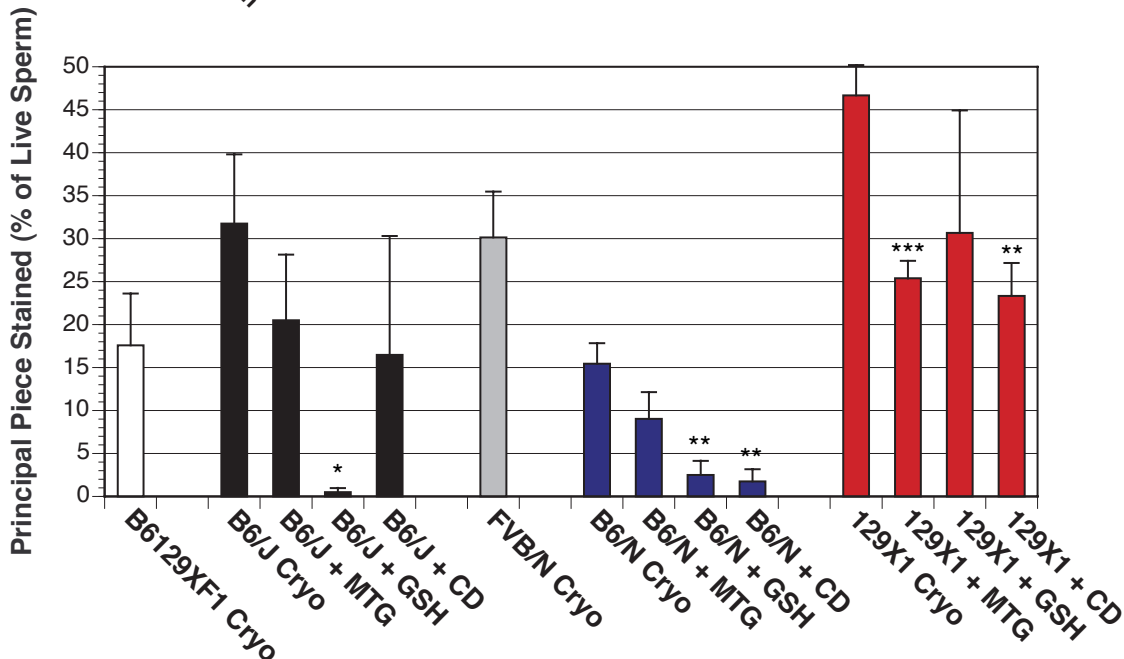
A



B

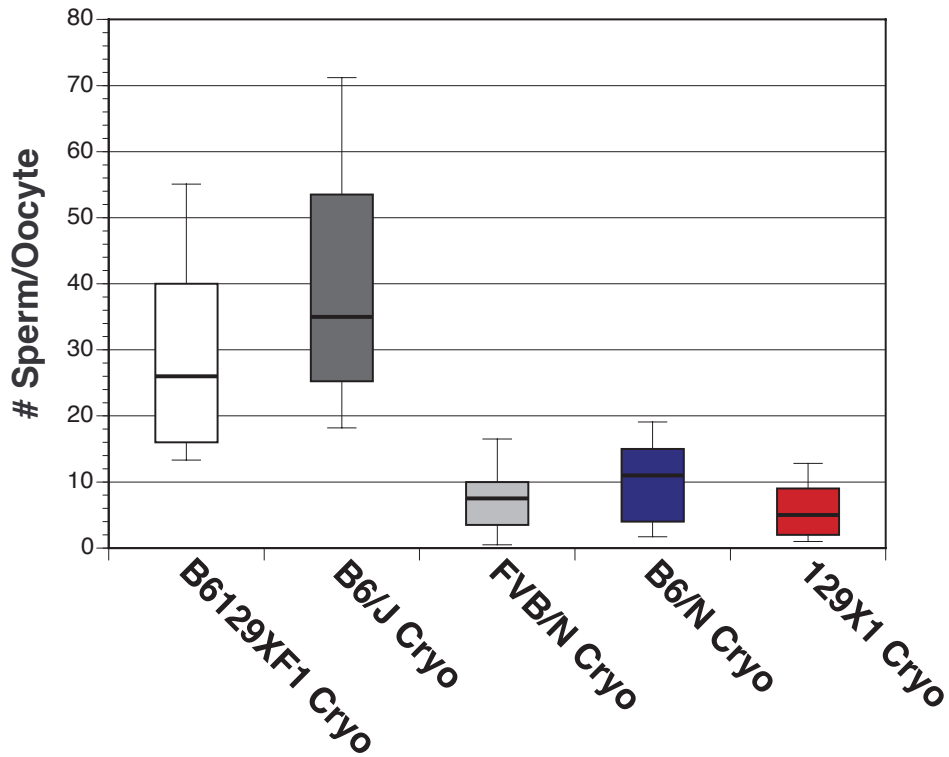


C

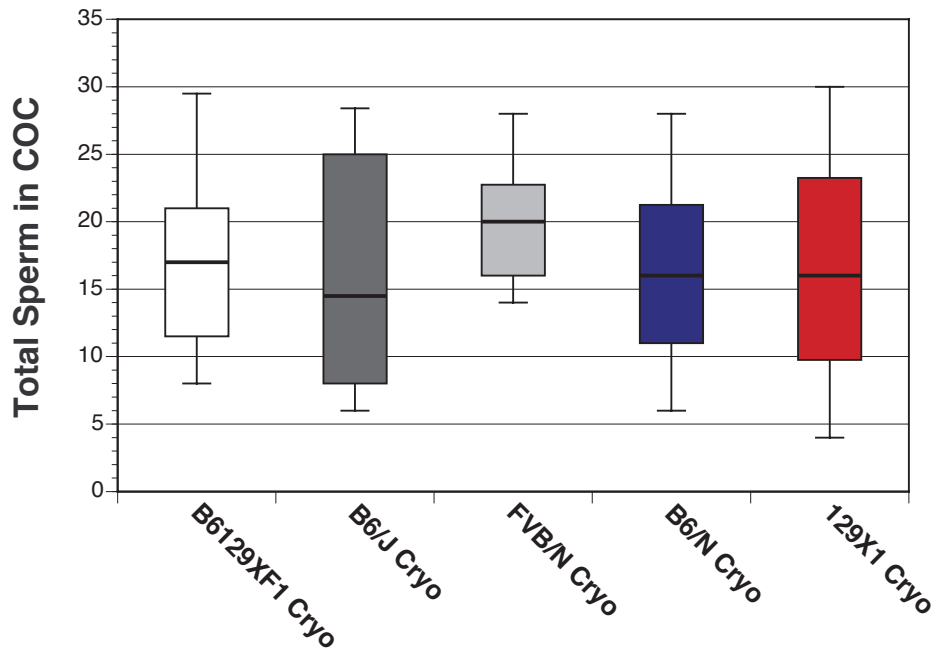


Supplemental Figure S4

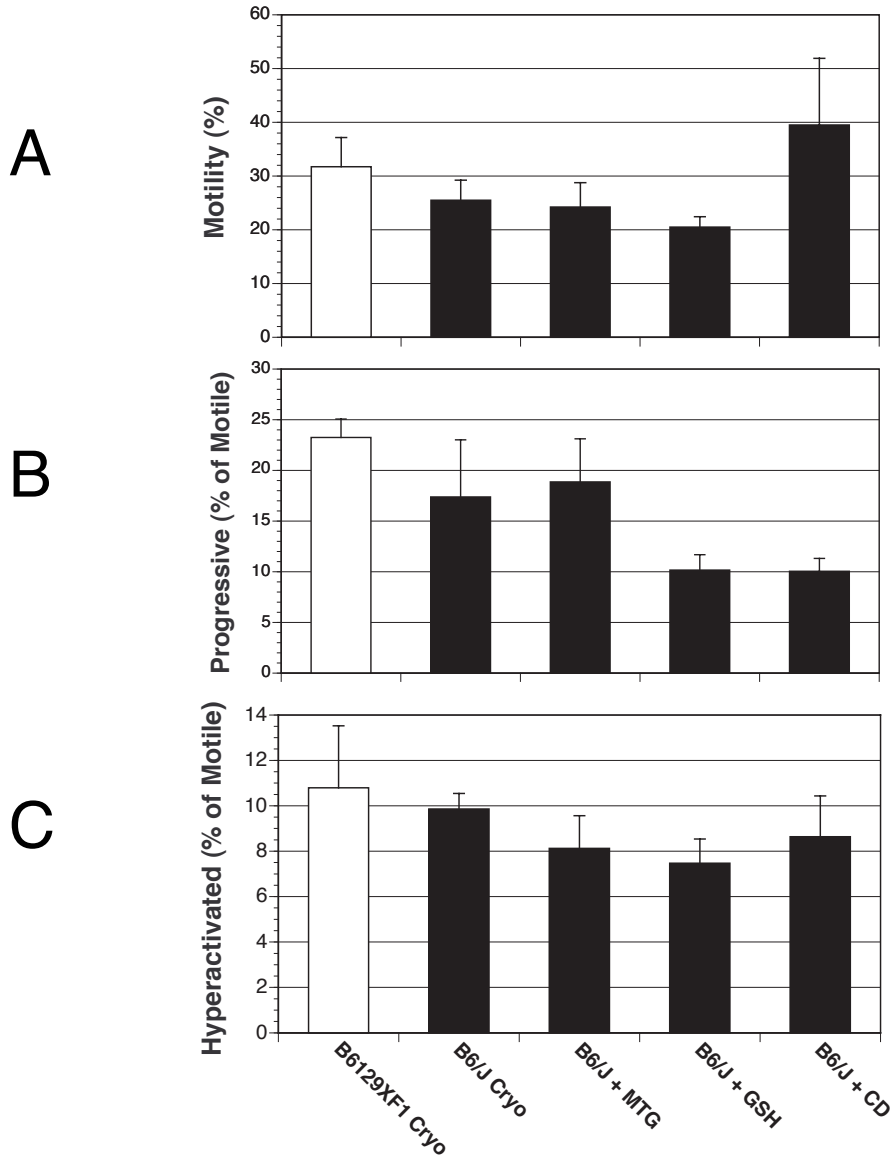
A



B

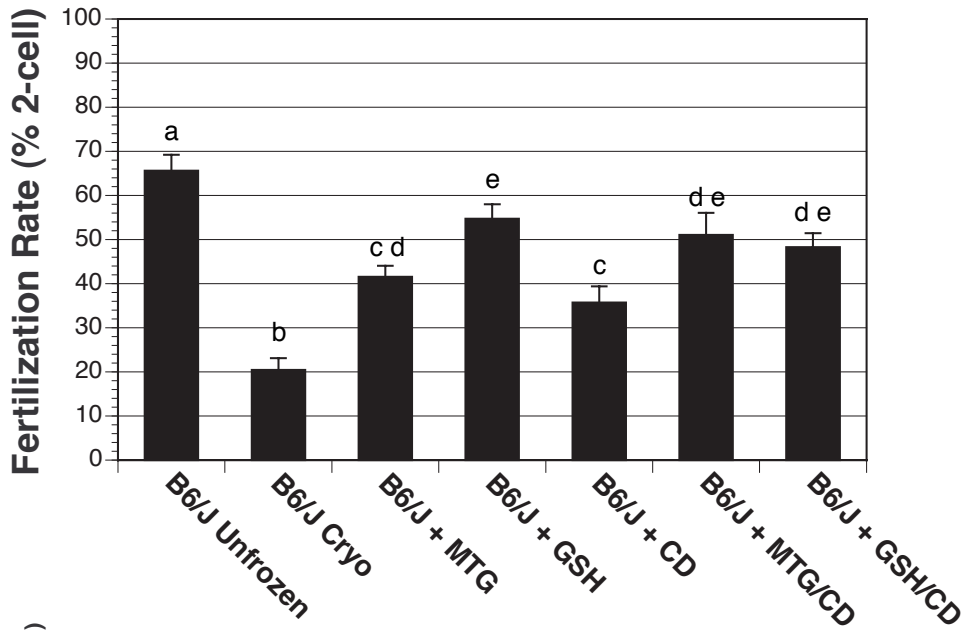


Supplemental Figure S5

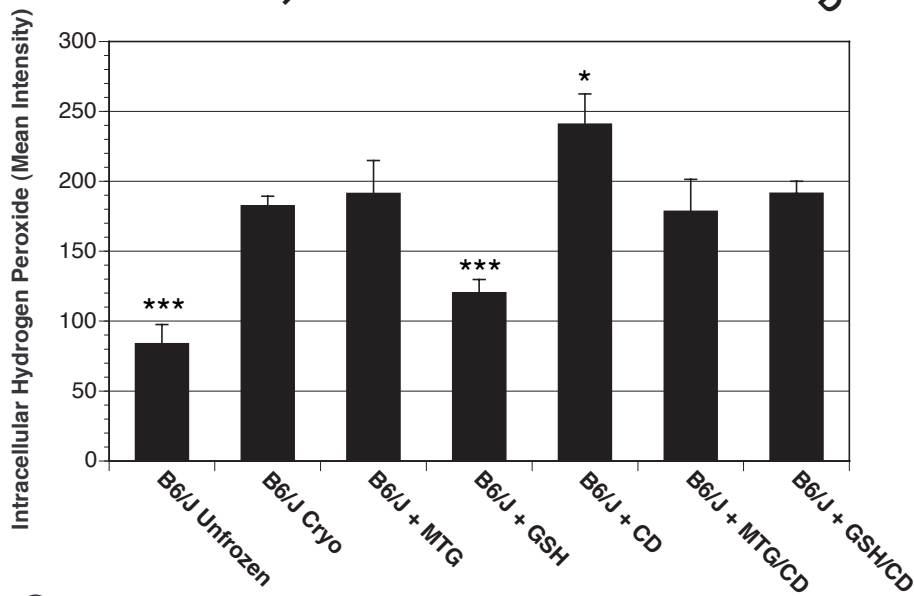


Supplemental Figure S6

A



B



C

